Accepted Manuscript

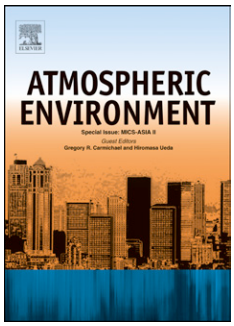

Volatile organic compound emissions from *Miscanthus* and short rotation coppice willow bioenergy crops

N. Copeland, J.N. Cape, M.R. Heal

PII: S1352-2310(12)00649-8

DOI: 10.1016/j.atmosenv.2012.06.065

Reference: AEA 11450

To appear in: *Atmospheric Environment*

Received Date: 29 March 2012

Revised Date: 18 June 2012

Accepted Date: 19 June 2012

Please cite this article as: Copeland, N., Cape, J.N., Heal, M.R., Volatile organic compound emissions from *Miscanthus* and short rotation coppice willow bioenergy crops, *Atmospheric Environment* (2012), doi: 10.1016/j.atmosenv.2012.06.065.

Volatile organic compound emissions from *Miscanthus* and short rotation coppice willow bioenergy crops

N. Copeland[1,2], J.N. Cape[1], M.R. Heal[2]

[1] Centre for Ecology & Hydrology, Bush Estate, Penicuik, EH26 0QB, UK

[2] School of Chemistry, University of Edinburgh, West Mains Road, Edinburgh, EH9 3JJ, UK

Corresponding author:

Dr Mathew R. Heal
School of Chemistry,
University of Edinburgh
West Mains Road
Edinburgh
EH9 3JJ, UK
Tel.: +44 (0)131 6504764
Email address: m.heal@ed.ac.uk

Abstract

Miscanthus x giganteus and short rotation coppice (SRC) willow (*Salix spp.*) are increasingly important bioenergy crops. Above-canopy fluxes and mixing ratios of volatile organic compounds (VOCs) were measured in summer for the two crops at a site near Lincoln, UK, by proton transfer reaction mass spectrometry (PTR-MS) and virtual disjunct eddy covariance. The isoprene emission rate above willow peaked around midday at ~1 mg m^{-2} h^{-1}, equivalent to 20 µg g_{dw}^{-1} h^{-1} normalised to 30°C and 1000 µmol m^{-2} s^{-1} PAR, much greater than for conventional arable crops. Average midday peak isoprene mixing ratio was ~1.4 ppbv. Acetone and acetic acid also showed small positive daytime fluxes. No measurable fluxes of VOCs were detected above the *Miscanthus* canopy. Differing isoprene emission rates between different bioenergy crops, and the crops or vegetation cover they may replace, means the impact on regional air quality should be taken into consideration in bioenergy crop selection.

Keywords: VOC, isoprene, bioenergy, *Miscanthus*, willow, eddy covariance

1 Introduction

Bioenergy crops are those grown specifically for energy production rather than food, as a means of mitigating two problems associated with the use of traditional fossil fuels: anthropogenic climate forcing and energy security (McKay, 2006). Such crops contribute to carbon neutrality since CO_2 produced during the combustion of the crop is offset by the CO_2 sequestered during growth. There is also potential for long-term storage of carbon via uptake by soil through plant roots (Grogan and Matthews, 2002). Consequently, cultivation of bioenergy crops is increasing rapidly. For example, power generators in the UK are required to increase to 15.4% by 2015/16 the energy derived from renewable sources (DTI, 2005), with biomass being acknowledged as a key resource in achieving this target.

Although bioenergy crops are perceived to be carbon neutral, full life-cycle analysis needs also to take account of changes in emissions of other potent greenhouse gases such as CH_4 or N_2O. Also, few studies have investigated volatile organic compound (VOC) emissions from bioenergy crops. Biogenic VOC emissions from vegetation (Steiner and Goldstein, 2007) are estimated as about 10 times greater globally than VOC emissions from anthropogenic sources (Guenther et al., 1995). The dominant BVOC is isoprene (Guenther et al., 2006), but other important compounds include oxygenated VOCs and terpenoids.

Emissions of VOCs are important for several reasons. Their rapid oxidation chemistry, particularly in the presence of NO_x, affects the oxidative capacity of the atmosphere, the generation of tropospheric ozone (Atkinson, 2000), of concern for human and plant health (Ashmore, 2005) and as a radiative forcing gas, and on formation of secondary organic

particles, which likewise affect human health (Dockery et al., 1993) and radiative forcing (Kulmala et al., 2004).

The potential for BVOC emissions from crops to have a significant impact on atmospheric composition has been demonstrated in the tropics (Hewitt et al., 2009). The aim of this study was to determine fluxes of BVOCs for two bioenergy crops grown in the UK and elsewhere: short rotation coppice (SRC) willow (*Salix spp.*), a woody crop grown in dense plantations of multi-stemmed plants and harvested every 3 years; and *Miscanthus x giganteus*, a perennial grass native to Asia, of the same taxonomic group as sugarcane, sorghum and maize (Naidu et al., 2003) but more resilient to lower temperature whilst maintaining high CO_2 assimilation and biomass conversion efficiency. The crop grows up to 3.5 m per year (Rowe et al., 2009), and is harvested annually between January and March. The chipped and dried biomass of both crops is used to fuel biomass burners or to co-fire existing coal-fired power stations.

Fluxes from this work are compared with those for conventional UK arable crops to assess the potential impact of this land-use change on atmospheric chemistry.

2 Methods

2.1 Sampling site

The field measurements were carried out from mid July to mid August 2010 near Lincoln, UK (53º 19′ N, 0º 35′ W). Figure 1 shows the layout of the site, which consisted of several fields of *Miscanthus*, willow and wheat, located within an area of predominantly flat arable fields separated by hedgerows and isolated areas of mixed deciduous woodland. Mean annual

rainfall at the site was 600 mm and the soil was a fine loam, overlying Charnmouth mudstone. The nearest settlement (population: 113), which had a relatively busy through-road, was ~0.7 km to the southeast. A minor road running east-west was situated 0.3 km to the south.

The *Miscanthus* plot (~11 ha, planted in spring 2006) was surrounded by the following vegetation types: hedgerow and wheat to the north; willow to the east; deciduous trees to the west; willow and wheat to the south. Crop height was typically 2.5 m. Sampling was carried out from 16th July to 2nd August 2010, near the NE corner of the plot, downwind of the prevailing wind direction, at an inlet height of approximately 4 m.

The willow plot (~6.5 ha, planted in 2001 with five different genotypes) was bounded as follows: a row of deciduous trees and a ploughed field to the north; *Miscanthus* to the west; mixed deciduous woodland to the south; wheat to the east. Typical canopy height was 4 m. Sampling was carried out from 5th to 13th August 2010 at an inlet height of 6.7 m on the north edge of the field. Trees were planted in pairs of rows 1.3 m apart, with 0.6 m spacing within each pair.

Flux footprints for both sampling sites were predicted using a simple parameterisation model (Kljun et al., 2004). Model results are shown in Supplementary Information Figure S1. For the *Miscanthus* measurements, the largest distance for 80% flux contribution over the range of friction velocities encountered (122 m) was within the area of the *Miscanthus* field throughout the south-westerly sector (180 – 270°). For the willow measurements, the largest distance for 80% flux contribution (185 m) meant there may have been some small flux contributions from outside the willow field when wind was from the west. Flux contribution was otherwise within the willow field for the whole southerly wind sector (90 – 270°). These sectors were used for

directional filtering of data prior to deriving diurnal averages. Directionally-filtered data comprised 23% and 71% of all data for *Miscanthus* and willow, respectively.

Harvesting activities in surrounding farms during this study may have affected results, particularly during *Miscanthus* measurements, and are discussed later.

2.2 Proton transfer reaction mass spectrometer (PTR-MS)

BVOC mixing ratios and fluxes above both crop canopies were measured using proton transfer reaction mass spectrometry (PTR-MS) (Blake et al., 2009) coupled with virtual disjunct eddy covariance (vDEC) (Karl et al., 2002; Rinne et al., 2001). PTR-MS is a 'soft' chemical ionisation method in which hydronium ions (H_3O^+) formed in a hollow cathode ion source pass into a drift tube subject to an electric field (E) into which the ambient air is also introduced. As most VOC molecules have a proton affinity greater than water, they react with H_3O^+ ions to form protonated products, predominantly the protonated molecular ion, but also fragments or clusters. The extent of fragmentation/clustering can be controlled by tuning the E/N ratio (N is the H_3O^+ ion density).

The PTR-MS used in this study (Ionicon Analytik, Innsbruck, Austria) was fitted with an extra turbopump connected to the detection chamber, and Teflon instead of Viton rings in the drift tube (Davison et al., 2009; Misztal et al., 2010). Pfeiffer turbopumps replaced the Varian equivalents. The drift tube conditions were held constant throughout (pressure 2 mbar, temperature 40 °C, voltage 572 V) to maintain an E/N ratio of ~130 Td (1 Td = 10^{-17} V cm^2).

The sampling inlet and 20 Hz sonic anemometer (WindmasterPro, Gill Instruments) were positioned above the canopy using a telescopic mast. Air was sampled at 30 L min^{-1} through a

20 m PTFE inlet line (1/4″ OD, 3/16″ ID) with a T-piece for sub-sampling into the PTR-MS inlet at a rate of 100 mL min^{-1}. Condensation of water vapour in the inlet line was prevented by wrapping with self-regulating heating tape (Omega, UK type SRF3-2C). Data were logged using a program written in LabVIEW (Version 8.5, National Instruments).

2.3 Determination of VOC mixing ratios and fluxes

The PTR-MS signal was calibrated explicitly for several VOCs using a mixed gas calibration cylinder (Apel-Riemer Environmental Inc., USA) containing 1 ppmv each of formaldehyde, methanol, acetonitrile, acetone, acetaldehyde, isoprene and 0.18 ppmv d-limonene. The calibration gas was diluted with VOC-scrubbed air to produce 6 samples with concentrations of 0.5, 1.0, 10, 20, 30 and 50% of the pure calibration gas standard. A relative transmission curve was then constructed to determine empirical calibration coefficients for other VOCs under study not present in the standard (Taipale et al., 2008). Calibrations were carried out in the lab before commencement of the field campaign, and on 22nd July during the campaign. Concentrations of gases in the calibration cylinder were verified using GC-MS calibrated with its own independent standards (details given in Section 2.4).

The PTR-MS was run in multiple ion detection (MID) mode for two 25 min sampling periods per hour. During these periods only the targeted VOC ions listed in Table 1 were measured, with dwell times of 0.5 s, in addition to the primary ion H_3O^+, and water cluster $(H_2O)H_3O^+$, which had dwell times of 0.2 s. The sensitivities (ncps $ppbv^{-1}$) and limits of detection (ppbv) for the target ions for the *Miscanthus* and willow campaigns are also included in Table 1. LODs were calculated as the ratio of twice the standard deviation of the background ion counts for a particular *m/z* throughout the campaign divided by the sensitivity (Karl et al., 2003).

158

159 The remaining 10 min per hour were used for full mass scans in the range 21 – 206 amu at a
160 dwell time of 1 s per amu. For one 5 min period, ambient air was scanned to allow information
161 about the full VOC composition to be acquired. For a further 5 min per hour, 'zero air' was
162 scanned to determine the instrument background. Zero air was achieved by sampling ambient
163 air through a custom-made zero-air generator comprising a glass tube packed with platinum
164 wool and a 50:50 mixture of platinum mesh and activated charcoal heated to 200°C. The
165 background spectrum was subtracted in subsequent processing of data.

166

167 As the PTR-MS was run in MID mode, fewer data points were generated than required for
168 direct eddy covariance due to the non-continuous manner in which the quadrupole mass
169 analyser measures each *m/z*. The set-up resulted in 30,000 wind speed measurements and up to
170 441 VOC measurements in each 25 min sampling period (depending on how many VOCs
171 were being measured). The total lag time between PTR-MS and wind speed data was
172 determined by examining the cross-correlation between vertical wind speed and VOC mixing
173 ratio as a function of lag time (with 15 s window). Total lag includes residence time in the
174 sampling inlet line but also lag associated with collection and data writing of a full cycle of
175 analysis by disjunct sampling and the response of the PTR-MS. The median of the lag times
176 for each 5 min sub-period was used to calculate the flux in that 25 min period (Misztal, 2010).
177 For example, the average lag-time for isoprene above the willow was 9.58 s, with a standard
178 deviation between 25 min periods of 1.41 s. This method produced less variable lag times than
179 those derived using the prevalent MAX method in cross-correlation function (~72% lower sd),
180 and has been shown to be a practical alternative (Taipale et al., 2010).

181

Quality controls were used to filter data for periods of low friction velocity (u^* <0.15 m s^{-1}), non-stationarity, large spikes in vertical wind speed or VOC concentration, and where <20000 data points were acquired in a 25 min sampling period. Most discarded data occurred during night when turbulence was low. High frequency flux losses due to the relatively slow disjunct VOC sampling frequency (0.25 Hz, compared to 20 Hz sonic data capture) were estimated using empirical ogive analysis (Ammann et al., 2006) for each 25 min period. At least 78% of flux was captured for all individual 25 min data periods, and values were corrected accordingly. Standard rotations of the coordinate frame were applied to correct for sonic anemometer tilt for each 25 min period separately.

2.4 Chromatographic analysis of ambient air samples

Ambient air samples were collected for chromatographic analysis, to confirm the identity of the VOC components measured by the PTR-MS, approximately hourly from 06:53 to 16:20 on 23 September 2010 above *Miscanthus* and from 06:32 to 17:30 on 11 August 2010 above willow (at ~1 m above the canopies). Sampling above *Miscanthus* was carried out at a later date because initial samples taken during the intensive campaign were lost due to GC-MS instrument failure. A mass-flow controlled Pocket Pump (210-1000 Series, SKC Inc.) was used to pump air at 100 mL min^{-1} for 15 min through stainless steel adsorbent tubes (6 mm OD) packed with 200 mg Tenax TA and 100 mg CarboTrap (Markes International Ltd., UK). Prior to sampling, packed tubes were conditioned at 300 °C for 15 min with a flow of helium.

Analyses were carried out using a Hewlett-Packard 5890/5970 GC-MS with an automated thermal desorption unit (ATD 400, Perkin Elmer) connected via a 200 °C heated transfer line. Transfer of samples from the adsorbent tubes was performed in two steps: heat to 280 °C for 5 min at 25 mL min^{-1} to desorb samples onto a Tenax-TA cold trap at −30 °C, followed by

transfer to the GC column at 300 °C for 6 min. Chromatographic separation utilised an Ultra-2 column (Agilent Technologies, 50 m × 0.2 mm ID × 0.11 µm film, 5% phenylmethyl silica) and a temperature program of 35 °C for 2 min, heat at 5 °C min^{-1} to 160 °C, heat at 10 °C min^{-1} to 280 °C, and hold for 5 min.

Calibration was carried out using a mixed monoterpene in methanol standard (10 ng μL^{-1} α-pinene, β-pinene, α-phellandrene, 3-carene and limonene (Sigma Aldrich, UK)) and an isoprene in nitrogen gas standard (700 ppbv, BOC Gases, UK). Aliquots of the monoterpene standard (0, 1, 3 and 5 µL) were injected onto 4 adsorbent tubes with helium carrier gas. Tubes continued to be purged with helium for 2 min after the standard injection. Isoprene calibration tubes were prepared by slowly (over a period of about 2 min) injecting 0, 10, 30 and 50 mL of the gas standard onto 4 adsorbent tubes, while purging with helium. The limits of detection for isoprene, α-pinene and limonene were 0.16, 0.23 and 0.30 ng on column, corresponding to mixing ratios of 38, 27 and 35 pptv, respectively, for a 1.5 L sample.

2.5 Meteorological measurements

Photosynthetically active radiation (PAR), rainfall, temperature and relative humidity were available as part of long-term measurements at the site.

3 Results

3.1 Miscanthus

The time series of VOC fluxes above *Miscanthus* are shown in Figure 2 along with u^* and sensible heat flux. Two periods of missing data 21st – 22nd and 25th – 27th July were due to

failure of the sampling pump. Data in the first few days were relatively noisy, showing no particular diurnal trend up to 20th July. This was likely due to elevated O_2^+ impurities during transport of the instrument resulting in less reliable primary ion counts or higher LOD. Additionally, episodes of rainfall on 17th, 18th, 20th and 22nd July may have resulted in a reduction in mixing ratio of VOCs where emission is proportional to PAR.

Small net emissions of isoprene and MEK from *Miscanthus* during daytime were just discernible, most noticeable on 18th July when sensible heat flux was also at its maximum. However, in general**,** flux data were somewhat noisy for all VOCs measured, and mostly not significantly different from zero. The directionally-filtered diurnal averages of VOC fluxes are shown in Supplementary Information Figure S2. As described earlier, the relevant sector for the *Miscanthus* measurements was south-west (180 – 270°). The mixing ratios of MVK+MACR (the first-generation oxidation products of isoporene) showed no diurnal pattern and were below LOD, so no data for these species are shown.

The time series of VOC mixing ratios above *Miscanthus* are shown in Supplementary Information Figure S3. For the period 27th July to 2nd August, mixing ratios of all measured VOCs had maxima at night except for isoprene whose mixing ratios were elevated in late afternoon. The average diurnal VOC mixing ratios above *Miscanthus* are shown in Figure S4. Methanol, acetaldehyde, acetone, acetic acid and MEK had similar diurnal profiles in mixing ratio. All showed a minimum mixing ratio around midday. The isoprene mixing ratio peaked around midday consistent with observation of a possible small isoprene flux above *Miscanthus* (Figure S2). No isoprene or monoterpenes were detected in the GC-MS analysis of adsorption tube sampling above the *Miscanthus* canopy.

256

257 *3.2 Short rotation coppice willow*

258 The time series of VOC fluxes, and u^* and sensible heat, measured above willow are shown in
259 Figure 3. Missing data on 10th and 12-13th August were due to failure of the mobile power
260 supply. Data were directionally filtered to include only those from over the willow field (90 –
261 270°) before diurnally averaging (Figure 4). Willow showed a distinct diurnal pattern of
262 isoprene flux, peaking at ~1 mg m^{-2} h^{-1} around midday and decreasing to zero overnight,
263 driven by the strong dependence of isoprene emissions on temperature and PAR. All other
264 VOC measured showed positive and negative fluxes throughout the day, with no significant
265 net positive or negative daily flux overall.

266

267 Supplementary Information Figure S5 shows the time series of VOC mixing ratios and
268 temperature above SRC willow. The time series showed clear diurnality in mixing ratios of all
269 VOCs measured, except for methanol. The directionally-filtered diurnal averages of mixing
270 ratio over the willow are shown in Figure 5.

271

272 Isoprene had a dominant maximum mixing ratio in early afternoon (~1 ppbv), temporally
273 coincident with the temperature profile, and low mixing ratios at night. Figure 5 also plots the
274 isoprene mixing ratios determined by adsorption tube sampling and GC-MS analysis. There
275 was good agreement. Small quantities of the monoterpenes α-pinene and limonene were also
276 detected by GC-MS, but no diurnal patterns were discernable in these data.

277

278 Acetic acid, acetaldehyde and MVK+MACR also showed diurnal profiles with maxima in the
279 afternoon and minima around 6 am, closely mirroring daily temperature variation. The
280 amplitude of the daytime maximum of MEK mixing ratio was considerably less. Acetone

281 exhibited low diurnal variability but with the small maximum in early morning similar to the
282 observation of *Miscanthus*.
283
284 As isoprene oxidation is the only known source of MVK and MACR, the ratio of
285 MVK+MACR to isoprene mixing ratios can be used to examine the degree of isoprene
286 oxidation (Figure 6). The [MVK+MACR]:[isoprene] ratio peaked around midnight with an
287 average value of about 0.8 when isoprene was not being emitted and MVK+MACR were not
288 undergoing photochemical loss or dispersion. At dawn there was a rapid decline in the ratio as
289 the canopy responded to increasing PAR and temperature hence isoprene emissions increased,
290 and the boundary layer depth also increased. The minimum ratio of ~0.1 occurred for several
291 hours around midday. The ratio rose in late afternoon as isoprene emissions declined but
292 isoprene oxidation continued.
293
294 The average measured daytime [MVK+MACR]:[isoprene] ratio of 0.24 is comparable with
295 those from other northern latitude studies. A daytime ratio of 0.23 was measured in a rural
296 Canadian forest clearing (Biesenthal et al., 1998), 0.12 was reported for a mixed forest in
297 Michigan, USA (Apel et al., 2002) and 0.4 – 0.8 in a deciduous forest in Pennsylvania, USA
298 (Martin et al., 1991).
299
300 *3.3 Standardised isoprene emission*
301 As isoprene emission from plants is strongly influenced by light and leaf temperature, the
302 canopy-level emission, *F*, was recalculated as a standard emission factor (ε) normalised to a
303 standard leaf temperature of 303 K and PAR flux of 1000 µmol m^{-2} s^{-1}, as described by the
304 G95 algorithm (Guenther et al., 1995),

$$\varepsilon = \frac{F}{D\,\gamma} \quad (1)$$

where D is foliar density (g dry weight m^{-2}) and γ is a non-dimensional activity adjustment factor to account for the effect of light and temperature:

$$\gamma = C_L C_T \quad (2)$$

The light dependence, C_L, is defined by

$$C_L = \frac{\alpha\, c_{L1}\, Q}{\sqrt{1 + \alpha^2 Q^2}} \quad (3)$$

where α (0.0027) and c_{L1} (1.066) are empirical coefficients and Q is PAR flux (µmol m^{-2} s^{-1}). The temperature dependence C_T, is defined by

$$C_T = \frac{\exp\frac{c_{T1}\,(T - T_s)}{R\,T_s\,T}}{1 + \frac{\exp\left(c_{T2}(T - T_M)\right)}{R\,T_s\,T}} \quad (4)$$

where T is leaf temperature (K), T_s is leaf temperature at standard conditions (303 K), R is the universal gas constant (8.314 J K^{-1} mol^{-1}), and c_{T1} (95000 J mol^{-1}), c_{T2} (230000 J mol^{-1}) and T_M (314 K) are empirical coefficients.

Values of above-canopy PAR and temperature, and of isoprene flux (from Figure 4), at hourly intervals during the willow campaign were used for the calculation of γ and F respectively. Foliar density D was estimated at 150 g_{dw} m^{-2} for *Salix spp.* (Karl et al., 2009). Hourly emission factors ε were then determined for isoprene from willow, and were found to have a peak value of 25 µg g_{dw}^{-1} h^{-1} at 10:00. A mean midday value of 20 µg g_{dw}^{-1} h^{-1} for 12:00 ± 2 h was determined to allow comparison, in Table 2, with mean values from other studies.

Table 2 shows that the emission factor from this study was within the range of values derived previously for *Salix spp*. The slightly lower measurements derived in this work and in the

other above-canopy study (Olofsson et al., 2005) were canopy-averaged emissions factors which included leaves which were in shade as well as those in direct sunlight. It was therefore expected that these measurements would result in lower standard emission factors than from individual branch or leaf-level experiments.

4 Discussion

In the context of SRC willow as a bioenergy crop, the significant isoprene emission factor could potentially impact local and regional air quality by affecting tropospheric ozone production and SOA formation. Conventional agricultural crops are regarded as being low emitting species. For example, wheat and oats are estimated as having isoprene emission factors in the range 0 - 0.5 $\mu g\ g_{dw}^{-1}\ h^{-1}$ (Karl et al., 2009; Konig et al., 1995), while those for rapeseed, rye and barley are zero (Karl et al., 2009; Kesselmeier and Staudt, 1999). Replacement of conventional crops with SRC willow would therefore result in increased isoprene emission. A recent study examined the impact of SRC crop cultivation in Europe (Ashworth et al., 2012). It was concluded that monthly mean increases in ozone and BSOA (+1% and +5% respectively) from low level planting scenarios were significant enough to affect regional air quality and therefore warrant consideration in short term local impact assessments, as well as life cycle analysis of bioenergy crops.

At the end of 2009, total UK plantings of *Miscanthus* and SRC willow were 12,700 and 6,400 ha respectively (DEFRA, 2009). A government report stated that there is potential in the UK to increase bioenergy crop cultivation substantially by a further 350,000 ha by 2020, accounting for ~6% of total UK arable land (DEFRA, 2007), with the assumption that 70%

352 would be *Miscanthus* and SRC willow (Rowe et al., 2009). In the case of 70% being converted
353 solely to SRC willow, then a UK-wide increase of up to 7.35 t h^{-1} in emissions of isoprene
354 would result (assuming zero isoprene emissions from the land prior to conversion to willow,
355 150 g_{dw} m^{-2} willow, and an isoprene standard emission rate of 20 µg g_{dw}^{-1} h^{-1} determined here).
356 The annual increase in isoprene would require calculation using PAR and temperature data
357 across the likely planting sites in the UK, and a whole-canopy model.
358
359 The standard emission factor for isoprene from SRC willow measured in this study was 26.5 g
360 C ha^{-1} h^{-1}. This is an order of magnitude higher than was determined for total emission of
361 VOCs from the biofuel crop switchgrass (Eller et al., 2011), where emissions were dominated
362 by oxygenated VOCs and isoprene contributed less than 8%.
363
364 For *Miscanthus*, the near-zero values of flux at night were in contrast to the increase in mixing
365 ratios of oxygenated VOCs (Figure S3 & S4). Since reliability of the eddy covariance
366 technique depends on friction velocity, the greater boundary layer stability at night (hence low
367 friction velocity) resulted in unreliable night time flux measurements. It may therefore be
368 possible that night time fluxes were non-zero. A more likely scenario is that increasing VOC
369 mixing ratios at night were affected by sources in the wider area. Towards the start of the
370 measurement period, several of the surrounding fields were subject to harvesting and
371 subsequent ploughing activities, which are known to be a source of oxygenated VOCs (Karl et
372 al., 2001). Mixing ratios of methanol, acetaldehyde and acetone were comparable to those
373 measured in previous field experiments of crop cutting (Warneke et al., 2002). The enhanced
374 mixing ratios towards dusk, and at night can be explained by reduced radical sink chemistry,
375 together with accumulation within a shallower nocturnal boundary layer from reduced vertical
376 transport and mixing, as demonstrated by the lower wind speed and u^* at night (Figure 2).

During willow measurements, atypical increases in mixing ratios of methanol, acetone and acetic acid on 8th August may also have been caused by further harvesting activity in the wider area.

5 Conclusions

Measurements of above-canopy fluxes and mixing ratios of VOCs revealed significant emissions of isoprene from short rotation coppice willow, with a standard emission factor of 20 µg g_{dw}^{-1} h^{-1}. No significant emissions were measured from *Miscanthus*. This is the first field study of bioenergy crops in the UK and shows that a change in land use from conventional to bioenergy crops could result in increased isoprene emissions. Bioenergy crop species choice should therefore include consideration of their impact on regional air quality. Further work could include measurement of VOC emissions from *Miscanthus* and SRC willow during senescence and harvesting.

Acknowledgements

N. Copeland acknowledges PhD studentship funding from EaStChem School of Chemistry and CEH Edinburgh. The authors thank Jonathan Wright and Frank Wilson for site access, Julia Drewer, Jon Finch and Eilidh Morrison for assistance with fieldwork set up, and Kirsti Ashworth and Catherine Hardacre for help with standard emission factors. We are also grateful to the anonymous reviewers of this paper for their helpful comments and suggestions.

400 **References**

401

402 Ammann, C., Brunner, A., Spirig, C., Neftel, A., 2006. Technical note: Water vapour
403 concentration and flux measurements with PTR-MS. Atmospheric Chemistry and Physics 6,
404 4643-4651.

405 Apel, E.C., Riemer, D.D., Hills, A., Baugh, W., Orlando, J., Faloona, I., Tan, D., Brune, W.,
406 Lamb, B., Westberg, H., Carroll, M.A., Thornberry, T., Geron, C.D., 2002. Measurement and
407 interpretation of isoprene fluxes and isoprene, methacrolein, and methyl vinyl ketone mixing
408 ratios at the PROPHET site during the 1998 Intensive. J. Geophys. Res. 107, 4034.

409 Ashmore, M.R., 2005. Assessing the future global impacts of ozone on vegetation. Plant Cell
410 and Environment 28, 949-964.

411 Ashworth, K., Folberth, G., Hewitt, C.N., Wild, O., 2012. Impacts of near-future cultivation of
412 biofuel feedstocks on atmospheric composition and local air quality. Atmospheric Chemistry
413 and Physics 12, 919 - 939.

414 Atkinson, R., 2000. Atmospheric chemistry of VOCs and NOx. Atmospheric Environment 34,
415 2063-2101.

416 Biesenthal, T.A., Bottenheim, J.W., Shepson, P.B., Li, S.M., Brickell, P.C., 1998. The
417 chemistry of biogenic hydrocarbons at a rural site in eastern Canada. J. Geophys. Res. 103,
418 25487-25498.

419 Blake, R.S., Monks, P.S., Ellis, A.M., 2009. Proton-Transfer Reaction Mass Spectrometry.
420 Chemical Reviews 109, 861-896.

421 Davison, B., Taipale, R., Langford, B., Misztal, P., Fares, S., Matteucci, G., Loreto, F., Cape,
422 J.N., Rinne, J., Hewitt, C.N., 2009. Concentrations and fluxes of biogenic volatile organic
423 compounds above a Mediterranean macchia ecosystem in western Italy. Biogeosciences 6,
424 1655-1670.

425 DEFRA, 2007. UK Biomass Strategy. DEFRA.

426 DEFRA, 2009. Experimental statistics. Non-food crop areas: United Kingdom. DEFRA.

427 Dockery, D.W., Pope, C.A., Xu, X.P., Spengler, J.D., Ware, J.H., Fay, M.E., Ferris, B.G.,
428 Speizer, F.E., 1993. An association between air-pollution and mortality in 6 United-States
429 cities. New England Journal of Medicine 329, 1753-1759.

430 DTI, 2005. Implementation guidance for the renewables obligation order 2005. DTI.

431 Eller, A.S.D., Sekimoto, K., Gilman, J.B., Kuster, W.C., de Gouw, J.A., Monson, R.K., Graus,
432 M., Crespo, E., Warneke, C., Fall, R., 2011. Volatile organic compound emissions from
433 switchgrass cultivars used as biofuel crops. Atmospheric Environment 45, 3333-3337.

434 Evans, R.C., Tingey, D.T., Gumpertz, M.L., Burns, W.F., 1982. Estimates of isoprene and
435 monoterpene emission rates in plants. Botanical Gazette 143, 304-310.

Grogan, P., Matthews, R., 2002. A modelling analysis of the potential for soil carbon sequestration under short rotation coppice willow bioenergy plantations. Soil Use and Management 18, 175-183.

Guenther, A., Hewitt, C.N., Erickson, D., Fall, R., Geron, C., Graedel, T., Harley, P., Klinger, L., Lerdau, M., McKay, W.A., Pierce, T., Scholes, B., Steinbrecher, R., Tallamraju, R., Taylor, J., Zimmerman, P., 1995. A global model of natural volatile organic compound emissions. Journal of Geophysical Research-Atmospheres 100, 8873-8892.

Guenther, A., Karl, T., Harley, P., Wiedinmyer, C., Palmer, P.I., Geron, C., 2006. Estimates of global terrestrial isoprene emissions using MEGAN (Model of Emissions of Gases and Aerosols from Nature). Atmospheric Chemistry and Physics 6, 3181-3210.

Hakola, H., Rinne, J., Laurila, T., 1998. The hydrocarbon emission rates of tea-leafed willow (Salix phylicifolia), silver birch (Betula pendula) and European aspen (Populus tremula). Atmospheric Environment 32, 1825-1833.

Hewitt, C.N., MacKenzie, A.R., Di Carlo, P., Di Marco, C.F., Dorsey, J.R., Evans, M., Fowler, D., Gallagher, M.W., Hopkins, J.R., Jones, C.E., Langford, B., Lee, J.D., Lewis, A.C., Lim, S.F., McQuaid, J., Misztal, P., Moller, S.J., Monks, P.S., Nemitz, E., Oram, D.E., Owen, S.M., Phillips, G.J., Pugh, T.A.M., Pyle, J.A., Reeves, C.E., Ryder, J., Siong, J., Skiba, U., Stewart, D.J., 2009. Nitrogen management is essential to prevent tropical oil palm plantations from causing ground-level ozone pollution. Proceedings of the National Academy of Sciences 106, 18447-18451.

Karl, M., Guenther, A., Koble, R., Leip, A., Seufert, G., 2009. A new European plant-specific emission inventory of biogenic volatile organic compounds for use in atmospheric transport models. Biogeosciences 6, 1059-1087.

Karl, T., Guenther, A., Jordan, A., Fall, R., Lindinger, W., 2001. Eddy covariance measurement of biogenic oxygenated VOC emissions from hay harvesting. Atmospheric Environment 35, 491-495.

Karl, T., Hansel, A., Märk, T., Lindinger, W., Hoffmann, D., 2003. Trace gas monitoring at the Mauna Loa Baseline Observatory using Proton-Transfer Reaction Mass Spectrometry. International Journal of Mass Spectrometry 223-224, 527-538.

Karl, T.G., Spirig, C., Rinne, J., Stroud, C., Prevost, P., Greenberg, J., Fall, R., Guenther, A., 2002. Virtual disjunct eddy covariance measurements of organic compound fluxes from a subalpine forest using proton transfer reaction mass spectrometry. Atmospheric Chemistry and Physics 2, 279-291.

Kesselmeier, J., Staudt, M., 1999. Biogenic volatile organic compounds (VOC): An overview on emission, physiology and ecology. Journal of Atmospheric Chemistry 33, 23-88.

Kljun, N., Calanca, P., Rotachhi, M.W., Schmid, H.P., 2004. A simple parameterisation for flux footprint predictions. Boundary-Layer Meteorology 112, 503-523.

Konig, G., Brunda, M., Puxbaum, H., Hewitt, C.N., Duckham, S.C., Rudolph, J., 1995. Relative contribution of oxygenated hydrocarbons to the total biogenic VOC emissions of

selected mid-European agricultural and natural plant-species. Atmospheric Environment 29, 861-874.

Kulmala, M., Suni, T., Lehtinen, K.E.J., Dal Maso, M., Boy, M., Reissell, A., Rannik, U., Aalto, P., Keronen, P., Hakola, H., Back, J.B., Hoffmann, T., Vesala, T., Hari, P., 2004. A new feedback mechanism linking forests, aerosols, and climate. Atmospheric Chemistry and Physics 4, 557-562.

Martin, R.S., Westberg, H., Allwine, E., Ashman, L., Farmer, J.C., Lamb, B., 1991. Measurement of isoprene and its atmospheric oxidation products in a central Pennsylvania deciduous forest. Journal of Atmospheric Chemistry 13, 1-32.

McKay, H., 2006. Environmental, economic, social and political drivers for increasing use of woodfuel as a renewable resource in Britain. Biomass & Bioenergy 30, 308-315.

Misztal, P., 2010. Concentrations and fluxes of atmospheric biogenic volatile organic compounds by proton transfer reaction mass spectrometry, EaStCHEM School of Chemistry. University of Edinburgh, Edinburgh.

Misztal, P.K., Owen, S.M., Guenther, A.B., Rasmussen, R., Geron, C., Harley, P., Phillips, G.J., Ryan, A., Edwards, D.P., Hewitt, C.N., Nemitz, E., Siong, J., Heal, M.R., Cape, J.N., 2010. Large estragole fluxes from oil palms in Borneo. Atmospheric Chemistry and Physics 10, 4343-4358.

Naidu, S.L., Moose, S.P., Al-Shoaibi, A.K., Raines, C.A., Long, S.P., 2003. Cold tolerance of C-4 photosynthesis in Miscanthus x giganteus: Adaptation in amounts and sequence of C-4 photosynthetic enzymes. Plant Physiology 132, 1688-1697.

Olofsson, M., Ek-Olausson, B., Jensen, N.O., Langer, S., Ljungström, E., 2005. The flux of isoprene from a willow coppice plantation and the effect on local air quality. Atmospheric Environment 39, 2061-2070.

Owen, S.M., Hewitt, C.N., 2000. Extrapolating branch enclosure measurements to estimates of regional scale biogenic VOC fluxes in the northwestern Mediterranean basin. Journal of Geophysical Research-Atmospheres 105, 11573-11583.

Pio, C.A., Nunes, T.V., Brito, S., 1993. Volatile hydrocarbon emissions from common and native species of vegetation in Portugal, in: Slanina, J., Angeletti, G., Beilke, S. (Eds.), Proceedings on the General Assessment of Biogenic Emissions and Deposition of Nitrogen Compounds, Sulfur Compounds and Oxidants in Europe, pp. 291-298.

Rinne, H.J.I., Guenther, A.B., Warneke, C., de Gouw, J.A., Luxembourg, S.L., 2001. Disjunct eddy covariance technique for trace gas flux measurements. Geophysical Research Letters 28, 3139-3142.

Rowe, R.L., Street, N.R., Taylor, G., 2009. Identifying potential environmental impacts of large-scale deployment of dedicated bioenergy crops in the UK. Renewable & Sustainable Energy Reviews 13, 260-279.

Steiner, A.H., Goldstein, A.L., 2007. Biogenic VOCs, in: Koppmann, R. (Ed.), Volatile Organic Compounds in the Atmosphere. Wiley-Blackwell, p. 512.

514 Taipale, R., Ruuskanen, T.M., Rinne, J., 2010. Lag time determination in DEC measurements
515 with PTR-MS. Atmospheric Measurement Techniques 3, 853-862.

516 Taipale, R., Ruuskanen, T.M., Rinne, J., Kajos, M.K., Hakola, H., Pohja, T., Kulmala, M.,
517 2008. Technical Note: Quantitative long-term measurements of VOC concentrations by PTR-
518 MS - measurement, calibration, and volume mixing ratio calculation methods. Atmospheric
519 Chemistry and Physics 8, 6681-6698.

520 Warneke, C., Luxembourg, S.L., de Gouw, J.A., Rinne, H.J.I., Guenther, A.B., Fall, R., 2002.
521 Disjunct eddy covariance measurements of oxygenated volatile organic compounds fluxes
522 from an alfalfa field before and after cutting. Journal of Geophysical Research-Atmospheres
523 107, 10.

524 Winer, A.M., Fitz, D.R., Miller, P.R., 1983. Investigation of the role of natural hydrocarbons
525 in photochemical smog formation in California. by the Statewide Air Pollution Research
526 Center, Riverside, California, U.S.A.

527 Zimmerman, P.R., 1979. Determination of emission rates of hydrocarbons from indigenous
528 species of vegetation in the Tampa/St. Petersburg Florida area. Appendix C. Tampa Bay area
529 photochemical oxidant study. U.S. Environmental Protection Agency, Region IV, Atlanta,
530 Georgia.
531
532
533

Miscanthus and coppice willow are increasingly important bioenergy crops.

Above-canopy fluxes were measured using PTR-MS and virtual disjunct eddy covariance.

Willow isoprene emission peaked at ~1 mg m^{-2} h^{-1}, ≡ 20 µg g_{dw}^{-1} h^{-1} standardised.

Bioenergy crop species choice should include their impact on regional air quality.

Table 1: Compounds measured during the field campaign including dwell times, sensitivities and limits of detection.

m/z [amu]	Contributing compound(s)	Formula	Dwell time [s]	Sensitivity [ncps ppbv $^{-1}$]	Limit of detection [ppbv]	
					Miscanthus	Willow
21	water isotope	$H_2{}^{18}O$	0.2	-	-	-
33	methanol	CH_4O	0.5	4.1	1.41	2.03
37	water cluster	$(H_2O)_2$	0.2	-	-	-
45	acetaldehyde	C_2H_4O	0.5	12	0.44	0.21
59	acetone propanal	C_3H_6O	0.5	11	0.41	0.06
61	acetic acid	$C_2H_4O_2$	0.5	10	0.08	0.06
69	isoprene furan methyl butenol fragment	C_5H_8	0.5	3.5	0.13	0.12
71	methyl vinyl ketone (MVK) methacrolein (MACR)	C_4H_6O	0.5	6.2	0.06	0.07
73	methyl ethyl ketone (MEK)	C_4H_8O	0.5	6.0	0.11	0.08

Table 2: Comparison of standardised emission rates of isoprene from willow. REA = relaxed eddy accumulation

Species	Standard emission rate / $\mu g\ g_{dw}^{-1}\ h^{-1}$	Measurement type	Reference
Salix spp.	20	Canopy-scale, PTR-MS	This study
Salix spp.	28	Branch enclosure	(Owen and Hewitt, 2000)
Salix alba	18	Branch enclosure, lab conditions	(Pio et al., 1993)
Salix alba	37.2	-	(Karl et al., 2009)
Salix babylonica	115	-	(Winer et al., 1983)
Salix caprea	18.9	Branch enclosure	(Karl et al., 2009)
Salix caroliniana	12.5	Air-exchange branch enclosure	(Zimmerman, 1979)
Salix nigra	25.2	Whole plant, air-exchange chamber	(Evans et al., 1982)
Salix phylicifolia	32	Branch enclosure	(Hakola et al., 1998)
Salix viminalis	12	Canopy-scale, REA	(Olofsson et al., 2005)

Figure captions

Figure 1: Aerial view of the Miscanthus and willow plantations. The white dots denote the measurement locations at the NE corner of the Miscanthus field and the N edge of the SRC willow field. (Map attributable to: ©2001 DigitalGlobe, GeoEye, Getmapping plc, Infoterra Ltd & Bluesky, TerraMetrics. Map data ©2011 Google).

Figure 2: Time series of VOC fluxes measured above Miscanthus. Dashed gridlines denote midnight. Note the variable flux scales.

Figure 3: Time series of VOC fluxes measured above willow canopy. Dashed gridlines denote midnight. Note the variable scales.

Figure 4: Average diurnal profiles of VOC fluxes above willow, and of sensible heat flux, when wind direction was between 90 and 270° (i.e. from over the willow field). Note the variable scales. Grey areas show variability calculated as ±1 sd of the averaged half-hourly values of all measurements.

Figure 5: Average diurnal profiles of VOC mixing ratios above willow, and of temperature, when wind direction was between 90 and 270° (i.e. from over the willow field). Note the variable scales. Dashed lines denote LOD. Grey areas represent variability calculated as ±1 sd of the averaged half-hourly values of all measurements.

Figure 6: Average diurnal profile of [MVK+MACR]:[isoprene] ratio above the willow canopy. Grey areas represent variability calculated as ±1 sd of the averaged half-hourly values of all measurements.

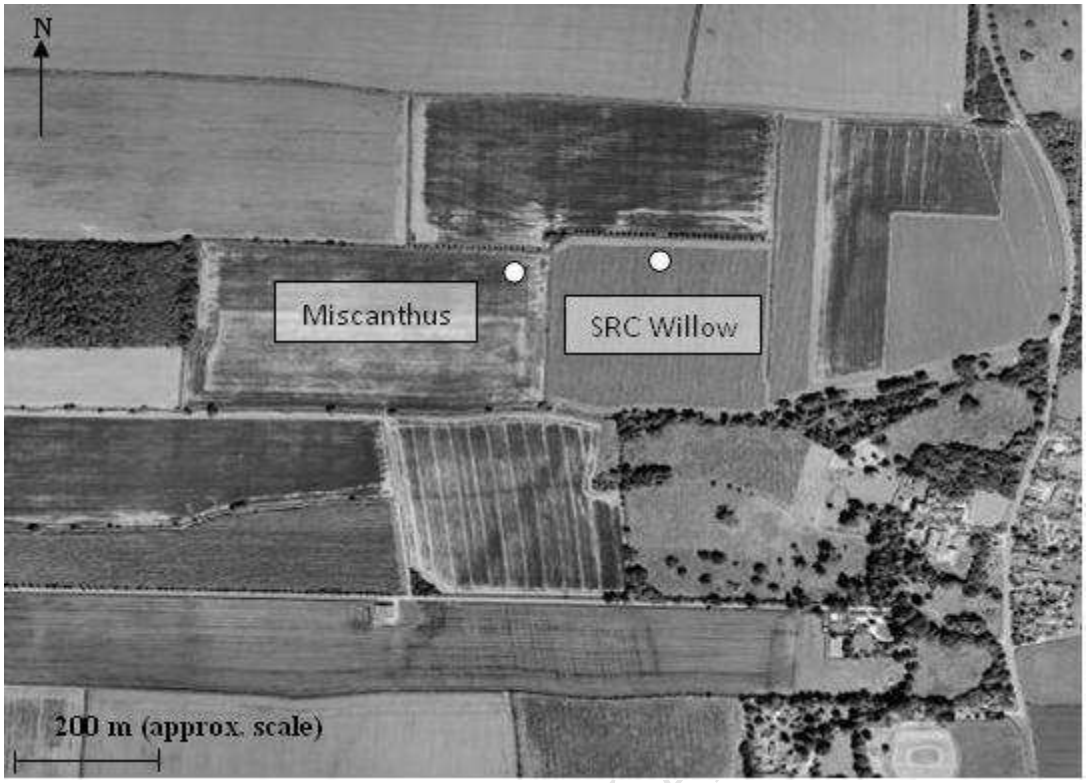

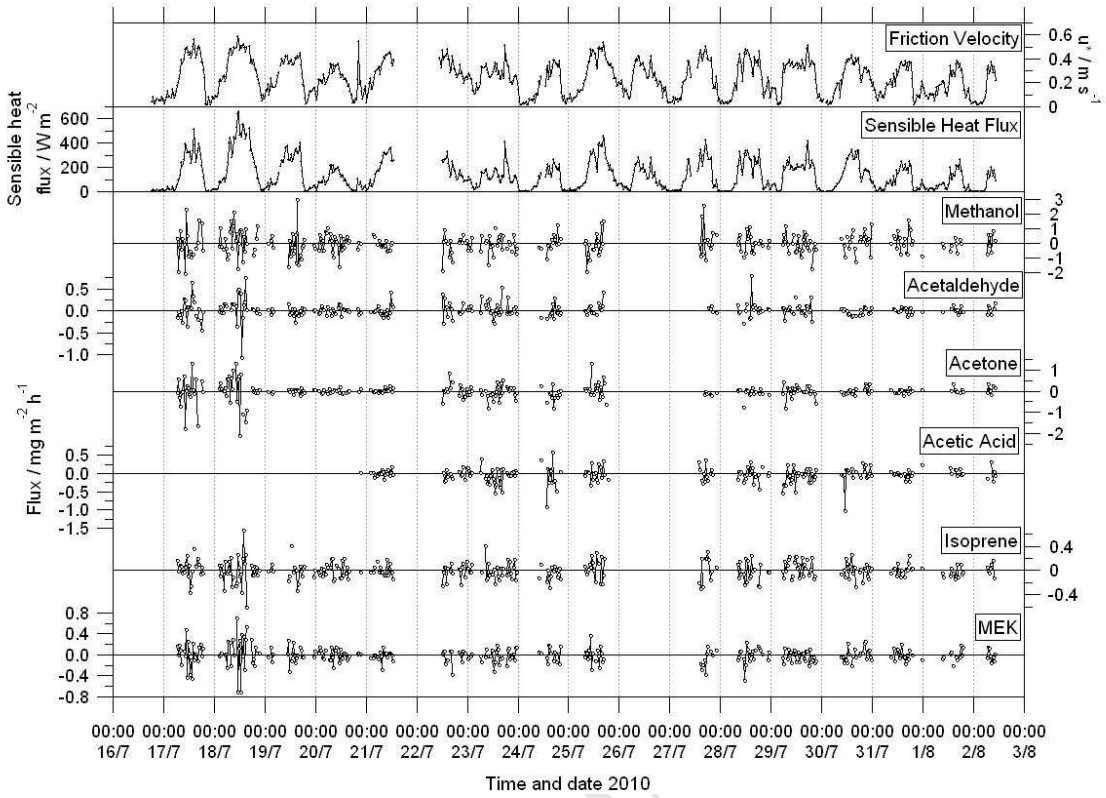

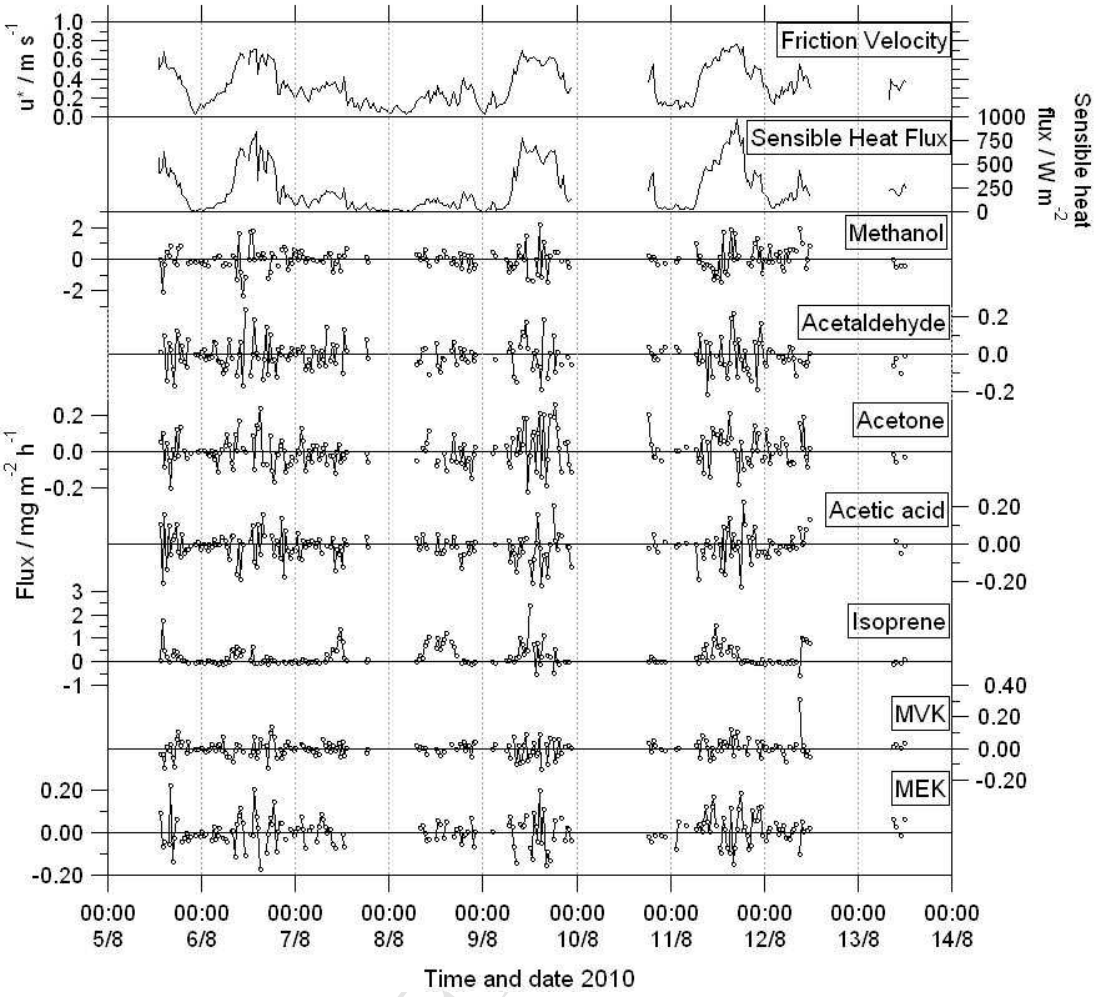

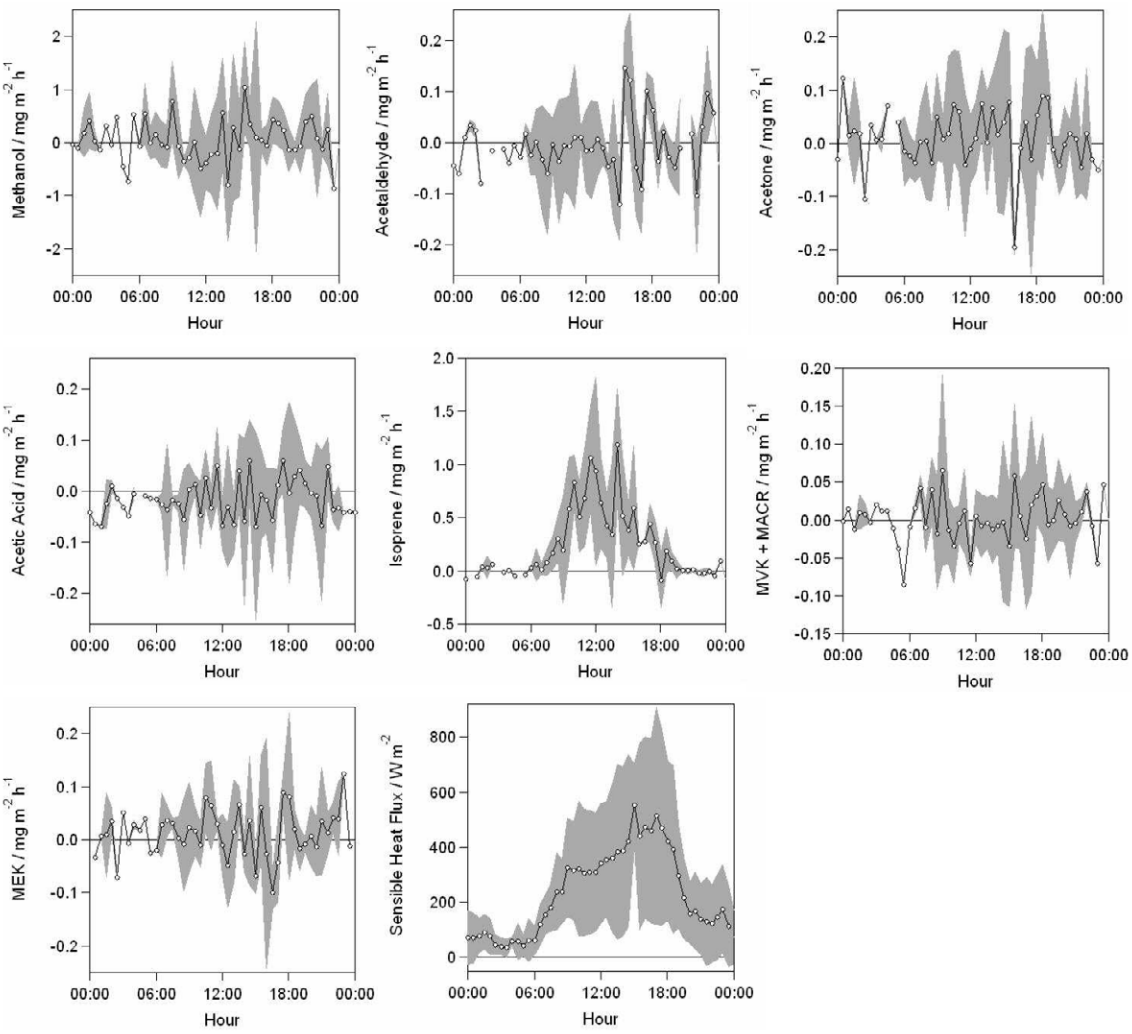
Methanol / mg m-2 h-1
Acetaldehyde / mg m-2 h-1
Acetone / mg m-2 h-1
Acetic Acid / mg m-2 h-1
Isoprene / mg m-2 h-1
MVK + MACR / mg m-2 h-1
MEK / mg m-2 h-1
Sensible Heat Flux / W m-2
00:00
06:00
12:00
18:00
00:00
Hour

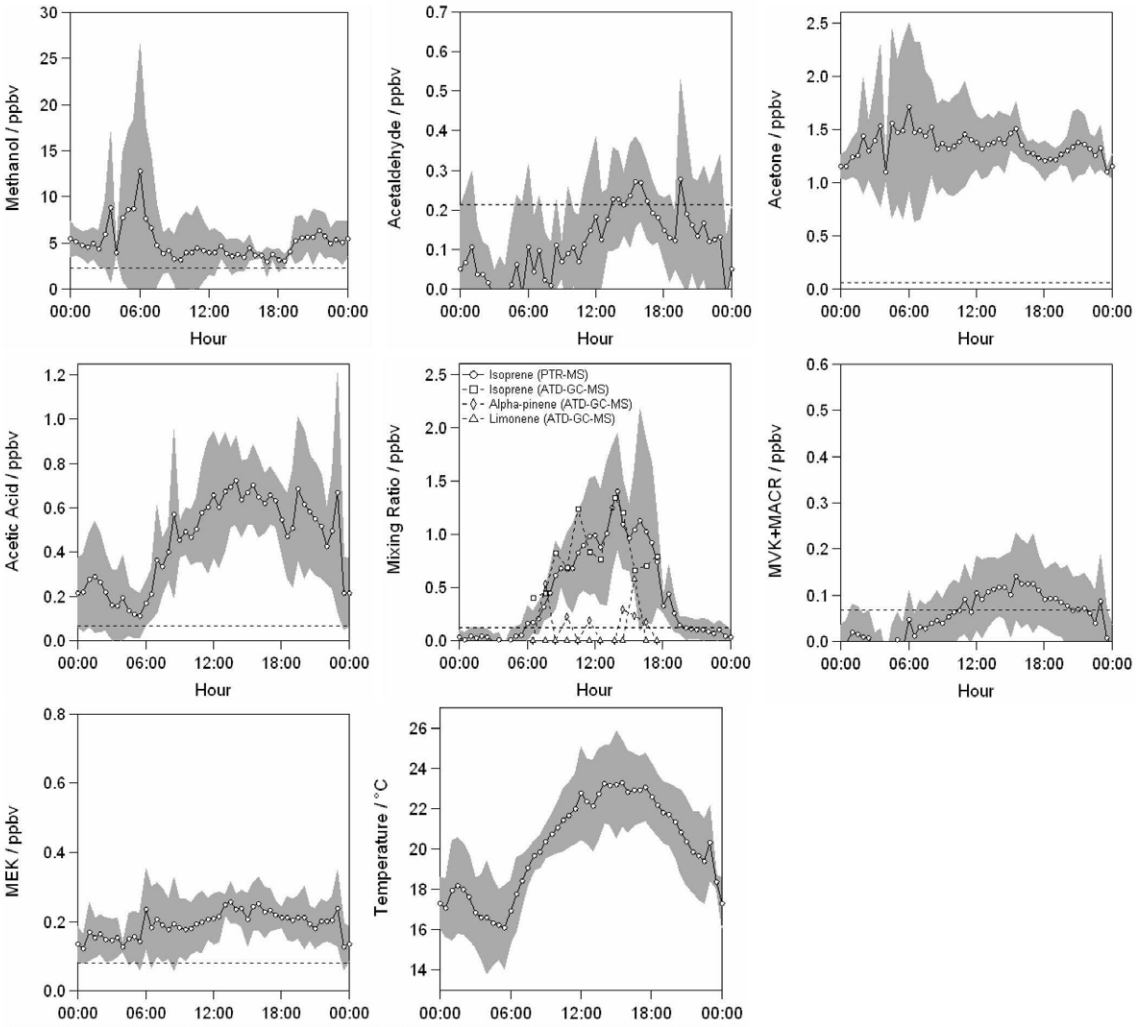
Methanol / ppbv
Acetaldehyde / ppbv
Acetone / ppbv
Acetic Acid / ppbv
Mixing Ratio / ppbv
Isoprene (PTR-MS)
Isoprene (ATD-GC-MS)
Alpha-pinene (ATD-GC-MS)
Limonene (ATD-GC-MS)
MVK+MACR / ppbv
MEK / ppbv
Temperature / °C
Hour
00:00
06:00
12:00
18:00

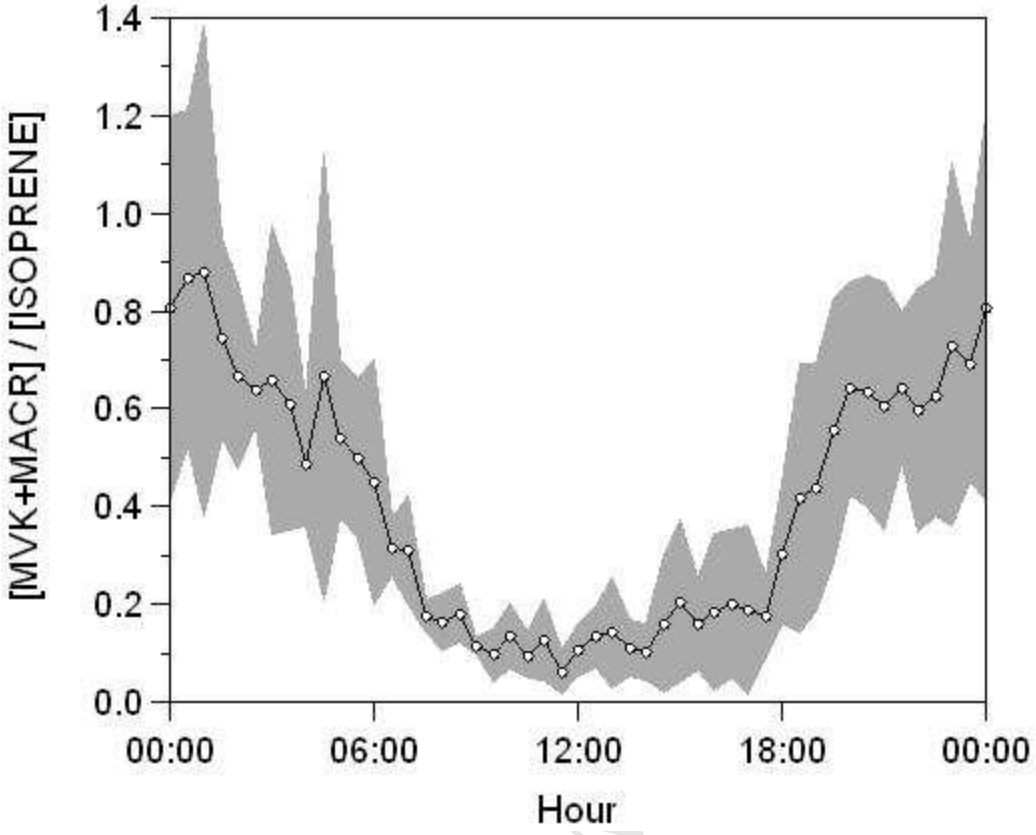

Supplementary Information

Volatile Organic Compound Emissions from *Miscanthus* and Short Rotation Coppice Willow Bioenergy Crops

N. Copeland[1,2], J.N. Cape[1], M.R. Heal[2]

[1] Centre for Ecology & Hydrology, Bush Estate, Penicuik, EH26 0QB, UK

[2] School of Chemistry, University of Edinburgh, West Mains Road, Edinburgh, EH9 3JJ, UK

The main paper reports on field measurements of VOC concentrations and fluxes above *Miscanthus* and short rotation crop (SRC) willow crops.

Average diurnal profiles were derived from the time series of measurements using data filtered to examine only those times when the wind direction and flux footprint was over the relevant crop field. The flux footprint for the range of friction velocities encountered was estimated as described in the main text, and the model output is shown here in Supplementary Information Figure S1. For measurements over *Miscanthus* and willow, directional filtering was undertaken for the sectors 180 – 270° and 90 – 270°, respectively. (See also the layout of the field site shown in Figure 1.)

Time series and directionally-filtered diurnal averages of both fluxes and mixing ratios of VOCs above both *Miscanthus* and SRC willow comprise too many figures to present in the main text. The most salient are presented in the main paper, and are mainly concerned with the measurements above SRC willow since measurements above *Miscanthus* showed essentially no significant VOC fluxes. For completion, the directionally-filtered diurnal averages of fluxes above *Miscanthus* are presented here in Figure S2, and the time series and directionally-filtered diurnal averages of the VOC mixing ratios above *Miscanthus* are presented in Figures S3 and S4, respectively. The time series of VOC mixing ratios above willow are shown in Figure S5.

Figure S1: Modelled flux footprints for *Miscanthus* and SRC willow measurements. The following parameters were used. *Miscanthus*: measurement height z_m 4 m; roughness length z_0 0.25 m (estimated as 1/10th of the canopy height, 2.5 m); boundary layer height *h* 1000 m. SRC willow: z_m 6.7 m; z_0 0.4m; *h* 1000 m. Footprints were calculated for 90th percentile (P90), median and minimum values of *u** (1 sd of the vertical wind speed, σ_w, shown in brackets) as indicated on the graphs. The distance at which maximum contribution can be expected, and at which 80% of the flux is contained, are given as X_{max} and X_r, respectively.

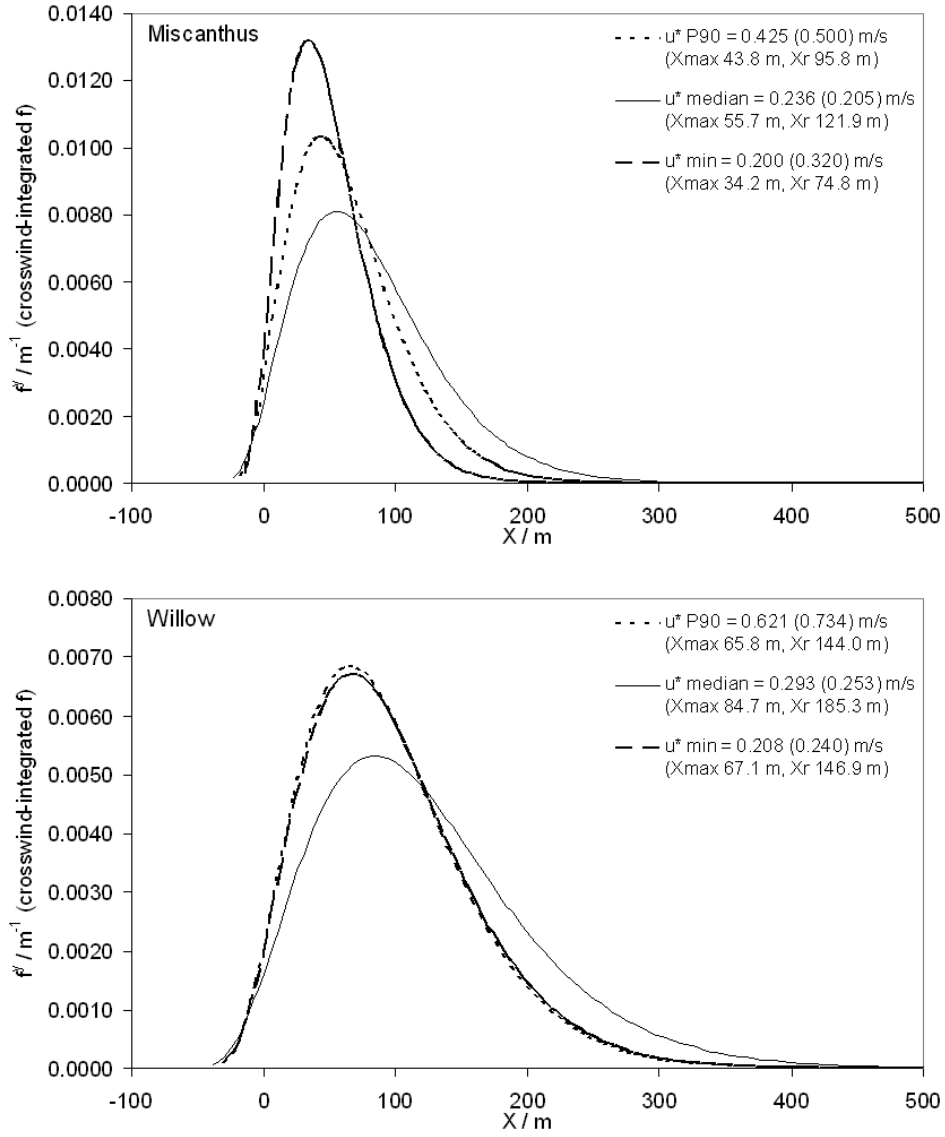

Figure S2: Average diurnal profiles of VOC fluxes above *Miscanthus* when wind direction was between 180 and 270° (i.e. from over the *Miscanthus* field). Note the variable scales. Grey areas represent variability calculated as ±1 sd of the averaged half-hourly values of all measurements. A profile for MVK+MACR is not included due to insufficient data.

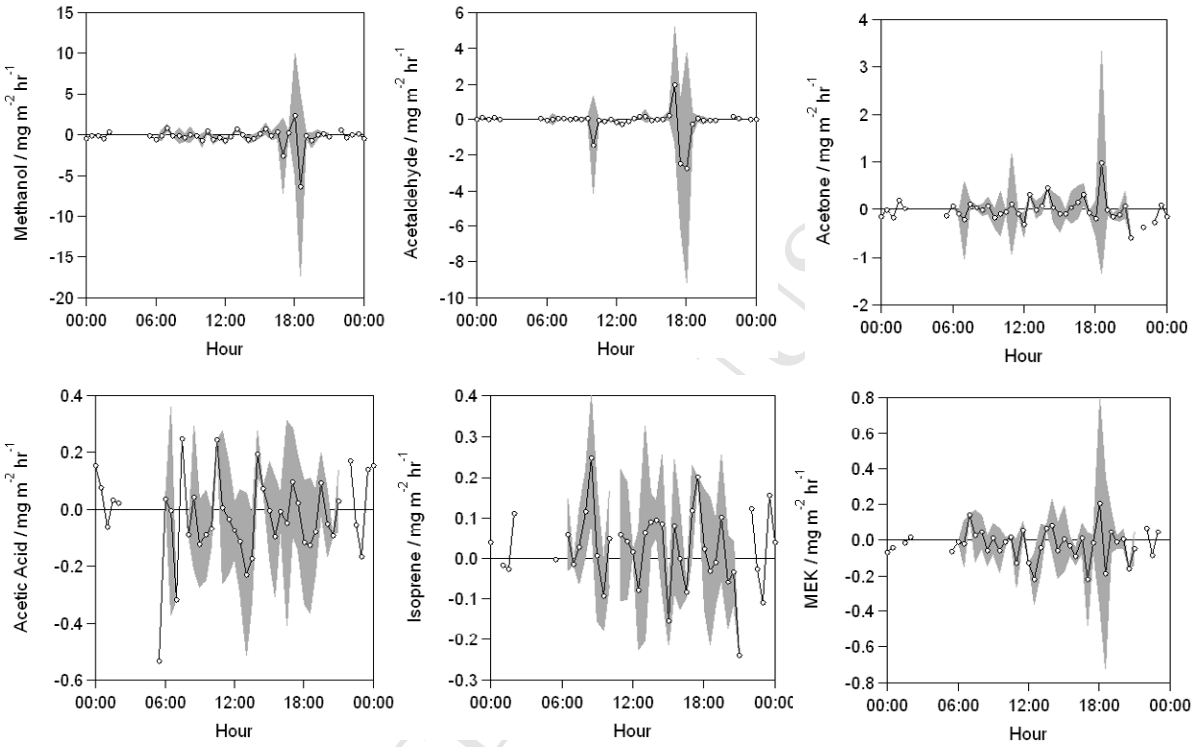

Figure S3: Time series of VOC mixing ratios, and of temperature, measured above *Miscanthus*. Dashed gridlines denote midnight. Note the variable mixing ratio scales.

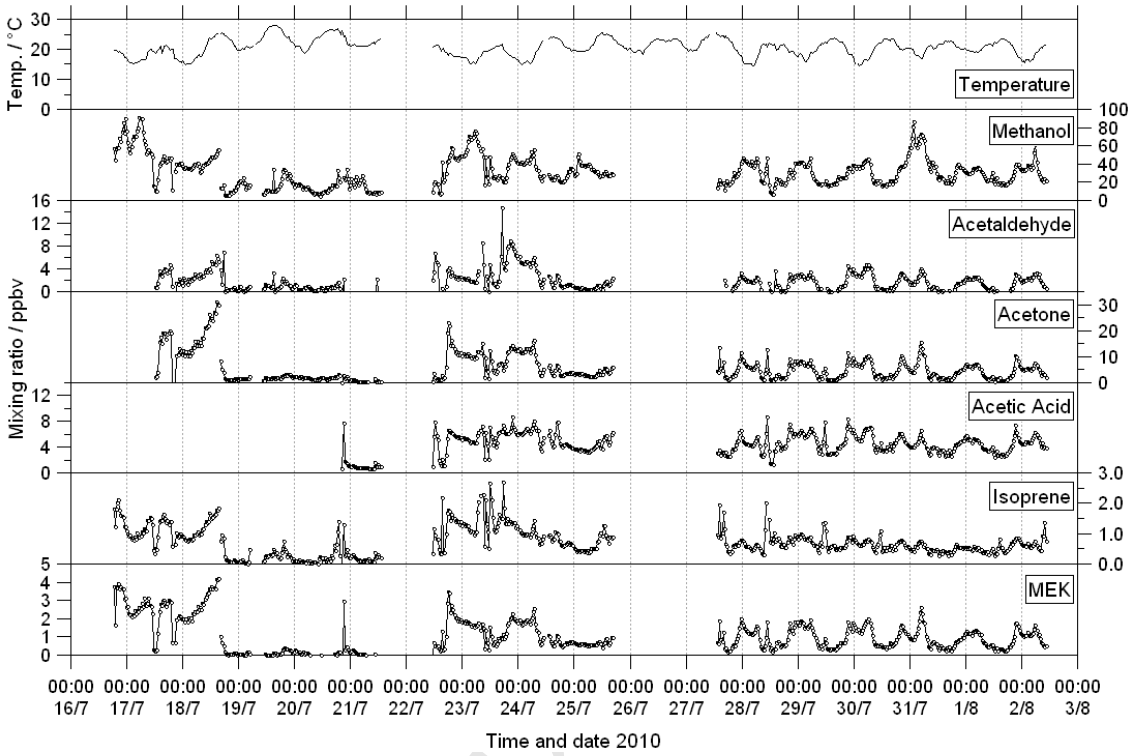

Figure S4: Average diurnal profiles of VOC mixing ratios above *Miscanthus*, and of temperature, when wind direction was between 180 and 270° (i.e. from over the *Miscanthus* field). Note the variable scales. Dashed lines denote LOD. Grey areas represent variability calculated as ±1 sd of the averaged half-hourly values of all measurements.

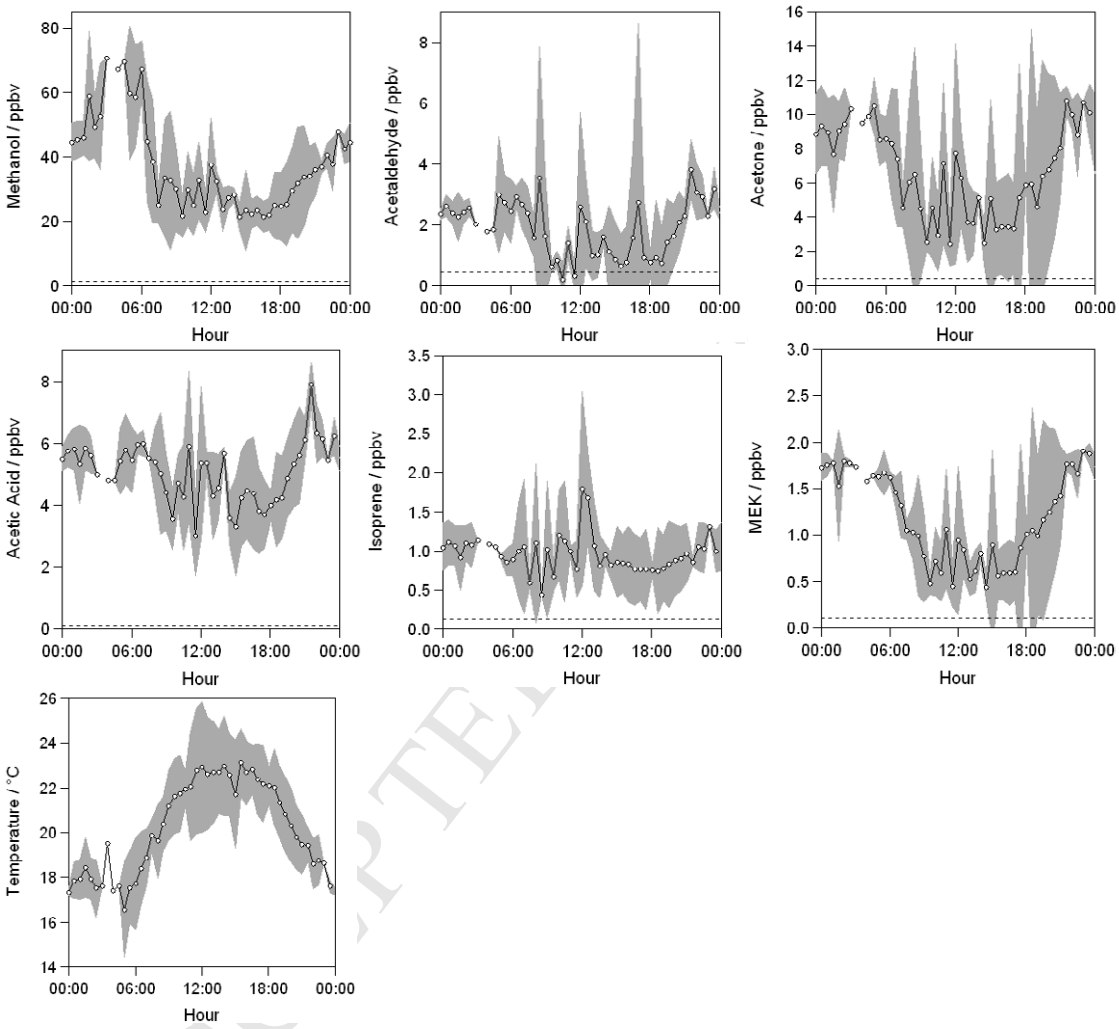

Figure S5: Time series of VOC mixing ratios, and of temperature, measured above willow. Dashed gridlines denote midnight. Note the variable mixing ratio scales.